

# The Reflection Coefficient of the Corundum-Based Material in X Band

M.G. Vakhitov\*<sup>(1)</sup>, D.S. Klygach<sup>(2)</sup>

(1) South Ural State University, Chelyabinsk, 76 Lenin Avenue, 454080, max\_v\_333@mail.ru

(2) South Ural State University, Chelyabinsk, 76 Lenin Avenue, 454080, klygachds@susu.ru

## Abstract

The paper describes the electrical properties of the composites consisting of polyurethane matrix dispersion- armoured with  $Al_2O_3$  grains. To prepare the materials, different corundum fractions were used. The dielectric permittivity of the materials was measured and the dielectric loss tangent was calculated in X band (8 – 12 GHz).

## 1. Introduction

Applying the ceramic face layer for producing various armour structures allows considerable improvement of their protection from the ordinary and armour-piercing bullets [1, 2]. This kind of materials is also more resistant to the high temperature long-term effects [3].

The technique of ceramics sintering is alternatively used in antenna engineering when producing the substrates for microstrip space-saving antennas [4] and in stealth technologies [5, 6]. Various additives for the materials and their effect on the mechanical and electrical properties in wide frequency range are considered amply in [7-9].

Carbon nanoparticles can be the additive, which influences the electrical properties of material and reflection coefficient. Polyurethane with variable content of carbon nanoparticles was applied on the cotton [10]. This kind of technology allows significant decreasing the reflection coefficient in X (8.2–12.4 GHz) band.

## 2. Problem Formulation

Most of the ceramic coatings are the plates with different shapes or thicknesses. Consequently, there are difficulties with protecting the long-sweep objects or objects with multiple asperities since the plates ought to fit a shape of the object to be protected. Otherwise, the coat could be made of small segments but in this case it is difficult to fix many small elements on the surface of the object.

To solve the problem of shaped objects, let us consider a material consisting of polyurethane matrix and corundum. Here polyurethane works as a base layer for a great number of corundum grains. Flexibility and plasticity of polyurethane resin provide coating of shaped objects.

In the investigation, the mixed size particles of  $Al_2O_3$  were used ranging from macroscopic ones (1-2 mm) to those nanoscaled (100 nm). To carry out the study, four samples of the material with different corundum concentrations and

particle sizes were prepared. The sample No. 1 taken for comparison was polyurethane resin without corundum additive.

Table 1 – Corundum concentration in the studied samples of the material

Sample No.	Mass concentration of corundum, %	Particle size in diameter, mm
1	-	-
2	63	0,001
3	75	1
4	70	1
5	73	1

## 3. Measurements

The investigation was performed by means of scanning electron microscope Jeol JSM-7001F. The surface was studied in a mode of secondary and reflected electrons and the maps of element distribution on the surface were constructed. Cross-sections of the developed composites were prepared for study.

X-ray fluorescence analysis was conducted by using the energy-dispersive spectrometer Oxford INCA X-max 80 set at the microscope. The spectrometer allows analysing the elements with atomic numbers from 5(B) to 92 (U).

Dielectric permittivity and dielectric loss tangent were measured using software and hardware appliance SPEAG that permits applying vector network analysers (VNA) for measuring electrical parameters of the materials.

## 4. Obtained Results

The obtained electron micrographs of sample cross-sections are demonstrated in Figure 1.

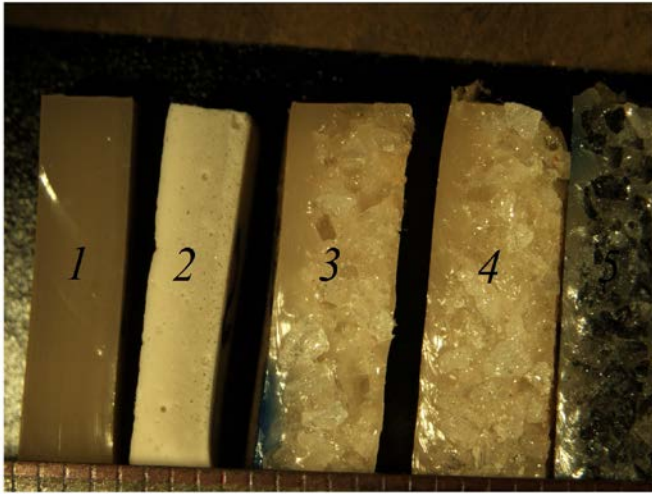


**Figure 1.** Cross-sections of the obtained material samples. 1 – sample No. 1; 2 – sample No. 2; 3 – sample No. 3; 4 – sample No. 4; 5 – sample No. 5.

A well-defined structure of composite material is noticed for all five samples in Figure 1. The structure of the 1<sup>st</sup> sample material, which is pure polyurethane, is homogeneous and the material does not include any foreign solids or air bubbles. The cross-sections of the samples 3 – 5 contain a great number of corundum grains filling maximally the available space while the polyurethane binder fills all the space between the grains. This improves the protective properties of a composite when penetrated with solid objects.

X-ray fluorescence analysis confirmed high purity of polyurethane and corundum used in the samples 2 – 4 (less than 0.5 mass % of impurities).

Corundum grains in the sample No. 5 are black and contain a small fraction of impurities giving the colour to corundum. Mass fractions of the impurity elements in the sample No. 5 are presented in Table 2.

Table 2 – Percentage of impurity mass fractions in the sample No. 5

Element	Ca	Ti	Mg	Fe	Cr
Mass fraction, %	6.2	3.5	0.8	0.5	0.2

The largest percentages of impurity mass fractions belong to Ca (6.5 %) and Ti (3.5%). Dependences of dielectric permittivity and dielectric loss tangent on frequency for the samples of the material are given in Figures 2 – 4.

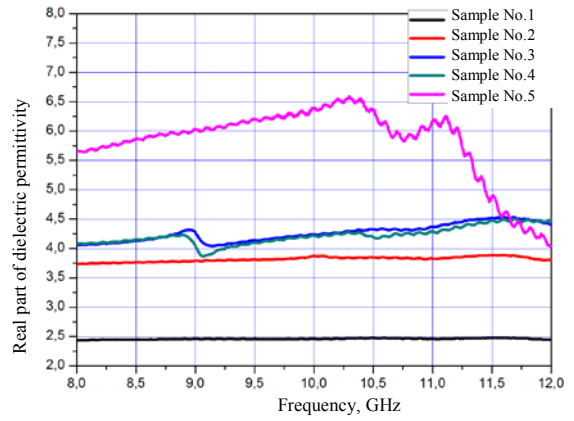


**Figure 2.** Real part of dielectric permittivity of material samples versus frequency

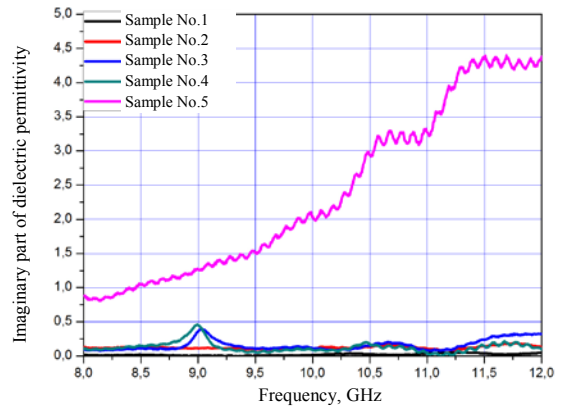


**Figure 3.** Imaginary part of dielectric permittivity of material samples versus frequency

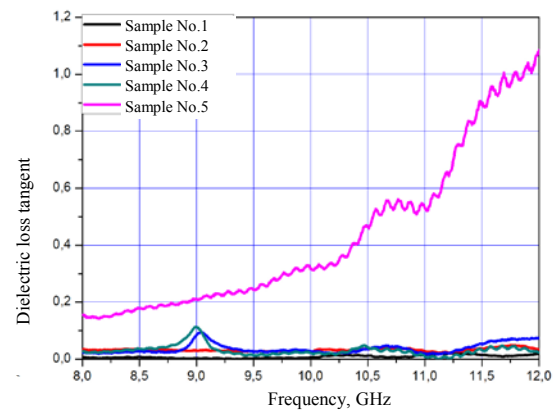


**Figure 4.** Dielectric loss tangent of material samples versus frequency

A reflection coefficient for electromagnetic waves reflecting from the material layer was calculated using the measured values of real and imaginary parts of dielectric and magnetic permittivity. Figures 5 – 9 present the dependences of the reflection coefficient on frequency for a different layer thickness.

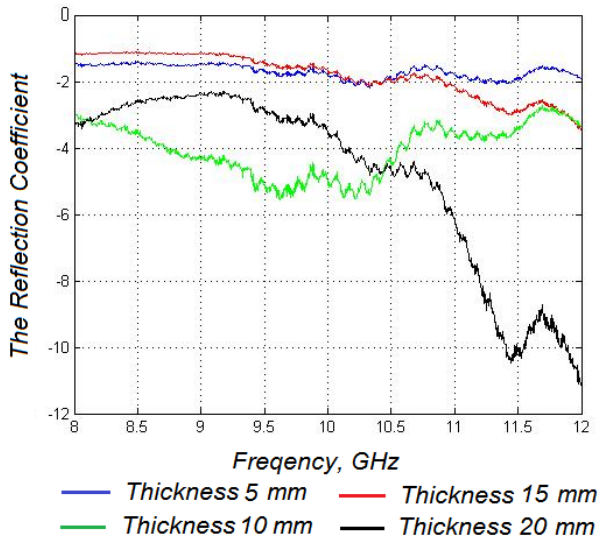


**Figure 5.** Dependences of the reflection coefficient on frequency for the 1<sup>st</sup> material sample

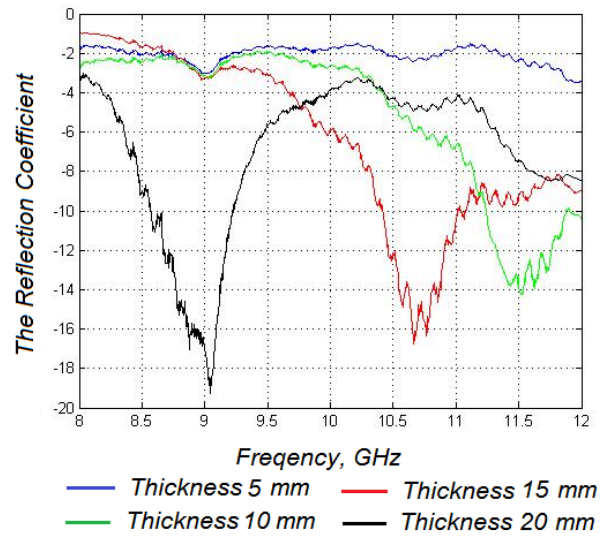


**Figure 8.** Dependences of the reflection coefficient on frequency for the 4<sup>th</sup> material sample

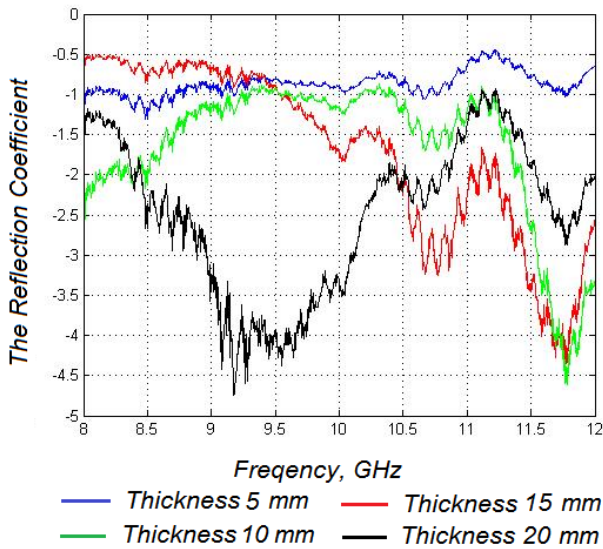


**Figure 6.** Dependences of the reflection coefficient on frequency for the 2<sup>nd</sup> material sample

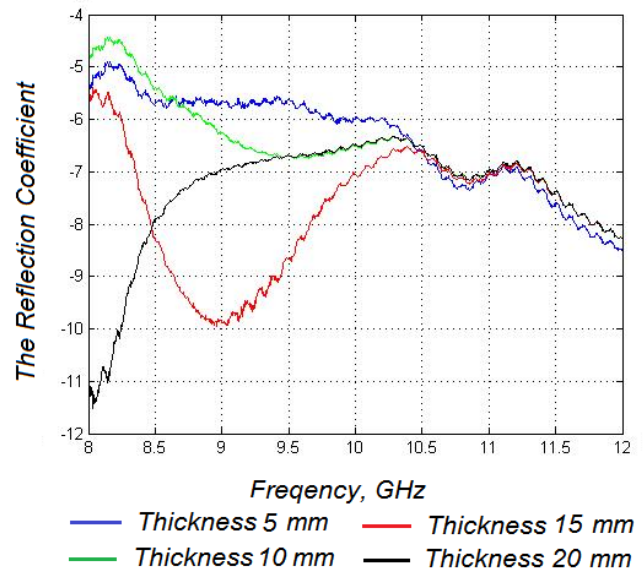


**Figure 9.** Dependences of the reflection coefficient on frequency for the 5<sup>th</sup> material sample

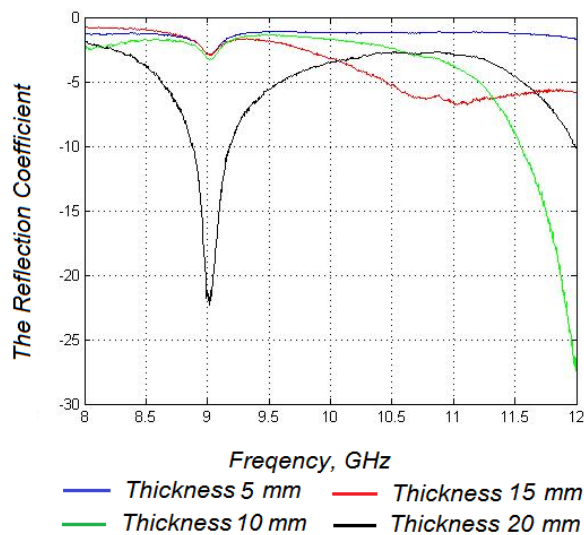


**Figure 7.** Dependences of the reflection coefficient on frequency for the 3<sup>rd</sup> material sample

## 5. Conclusions

Introduction of the corundum grain impurity with a particle diameter less than 100 nm (sample No. 2) results only in growth of dielectric permittivity up to the value  $\epsilon_2=3.75$  in the frequency range for the obtained material, in comparison with that  $\epsilon_1=2.5$  for pure polyurethane.

Utilization of the refined corundum grains with a particle diameter 1 mm leads not only to enhancement of the material protective properties but also to a growth of dielectric permittivity versus frequency  $\epsilon_{3,4}=4.25$ . Besides, the obtained samples No. 1 and 2 show linear dependence of dielectric permittivity on frequency while the dependence of dielectric permittivity on frequency for the samples 3–5 with the increased corundum concentration is non-linear.

The use of unrefined corundum with the grain impurities, 1 mm in diameter, leads to increasing dielectric permittivity in the frequency range and its non-linear dependence on

frequency. The sufficient growth of dielectric loss tangent can be explained by dispersion properties of the obtained material. The major dielectric losses are due to the impurities of Ca and Ti in the material of the sample No. 5.

Since the obtained material has high losses in the studied frequency band, it can be applied as a radar absorbing material in X band. Electromagnetic wave will damp considerably during its propagation in the material of the sample No. 5 due to high values of imaginary part of dielectric permittivity and dielectric loss tangent. Varying the thickness of the material samples makes it possible to obtain the reflection coefficient value up to  $-16$  dB due to the losses in the material.

## 6. Acknowledgment

The work was supported by Act 211 Government of the Russian Federation, contract 02.A03.21.0011.

## 7. References

1. Kharchenko E.F., Ermolenko A.F. Composite, textile and combined armor materials. Moscow: Publ. of TsNIISM, 2014. 332 p.
2. Grigorian V.A., Kobylkin I.F., Mirinin V.M., Chistyakov E.N. Materialy i zashchitnye struktury dlya lokal'nogo i individual'nogo bronirovaniya. Moscow: RadioSoft, 2008. 406 p.
3. Bobić, J.D., Vijatović Petrović, M.M., Banys, J., Stojanović, B.D. Electrical properties of niobium doped barium bismuth-titanate ceramics (2012) *Materials Research Bulletin*, 47 (8), pp. 1874-1880.
4. De Arimateia Pinto Magno, J., De Andrade, H.D., De Souza Queiroz, I., Maia, A.S., De Almeida Silveira, J.H., De Souza, D. A proposal of a ceramic material ( $\text{Nb}_2\text{O}_5$ ) for applications in microstrip antenna substrates (2015) *SBMO/IEEE MTT-S International Microwave and Optoelectronics Conference Proceedings*, 2015-December, art. no. 7369092.
5. Balci, O., Polat, E.O., Kakenov, N., Kocabas, C. Graphene-enabled electrically switchable radar-absorbing surfaces (2015) *Nature Communications*, 6, art. no. 6628.
6. Tian, L., Yan, X., Xu, J., Wallenmeyer, P., Murowchick, J., Liu, L., Chen, X. Effect of hydrogenation on the microwave absorption properties of  $\text{BaTiO}_3$  nanoparticles (2015) *Journal of Materials Chemistry A*, 3 (23), pp. 12550-12556.
7. Subohi, O., Bowen, C.R., Malik, M.M., Kurchania, R. Dielectric spectroscopy and ferroelectric properties of magnesium modified bismuth titanate ceramics (2016) *Journal of Alloys and Compounds*, 688, pp. 27-36.
8. Subohi, O., Singh, R., Kumar, G.S., Malik, M.M., Kurchania, R. Impedance analysis and dielectric properties of Ce modified bismuth titanate lead free ceramics synthesized using solution combustion route (2015) *Journal of Materials Science: Materials in Electronics*, 26 (11), pp. 9122-9133.

9. Yoon, S.-H., Hong, M.-H., Hong, J.-O., Kim, Y.-T., Hur, K.-H. Effect of acceptor (Mg) concentration on the electrical resistance at room and high (200 °C) temperatures of acceptor (Mg)-doped  $\text{BaTiO}_3$  ceramics (2007) *Journal of Applied Physics*, 102 (5), art. no. 054105.

10. Gupta, K.K., Abbas, S.M., Abhyankar, A.C. Carbon black/polyurethane nanocomposite-coated fabric for microwave attenuation in X & Ku-band (8–18 GHz) frequency range (2016) *Journal of Industrial Textiles*, 46 (2), pp. 510-529.

11. Vakhitov M.G. Application of radar absorbing coatings for reduction of effective scattering surface. *Bulletin of the South Ural State University Series "Computer Technologies, Automatic Control, Radio Electronics"* 2015, vol. 15, no.1, pp.139–144.